

Vapreotide-modified nanomicelle as a targeted nanocarrier for delivering paclitaxel to the tumors with overexpression of somatostatin receptors

Wenjie Hou, Hua Zheng, Jiancheng Wang*

Department of Pharmaceutics, School of Pharmaceutical Sciences, Peking University Health Science Center, Beijing 100191, China

Abstract: Somatostatin receptors (SSTRs) were widely expressed in many tumor cells. As a somatostatin analogue, vapreotide (VAP) can be exploited as a modifier for targeting tumor therapy based on its high affinity to SSTR. In this study, we conjugated α -NH₂ of exocyclic D-phenylalanine (D-Phe) of vapreotide to *N*-hydroxysuccinimidyl-PEG₂₀₀₀-DSPE (NHS-PEG-DSPE), and the resulted DSPE-PEG-VAP was used as a targeting component to construct the targeted micelles for delivering paclitaxel (VAP-M-PTX) through a thin-film hydration method. Similar particle size, zeta potential, drug encapsulation efficiencies, drug release behaviors and hemolysis effects were observed between the targeted micelles (VAP-M-PTX) and the non-targeted micelles (M-PTX). In MCF-7 cells, significantly higher intracellular fluorescence intensity (1.5-fold) was determined by flow cytometry after incubation of coumarin-6 loaded targeted micelles (VAP-M-Cou) for 3 h compared with non-targeted micelles (M-Cou), and similar finding was observed confocal microscopy. Furthermore, in comparison with non-targeted formulations, higher antitumor efficacy and higher drug accumulation were found in MCF-7 tumors in nude mice after intravenous injection of the targeted micelles. In conclusion, we believed that the vapreotide-modified nanomicelles could be a promising targeted nanocarrier for delivering anticancer drugs to the tumors with overexpression of somatostatin receptors.

Keywords: Somatostatin receptor, Vapreotide, Targeted nanomicelle, Paclitaxel, Tumor therapy

CLC number: R945

Document code: A

Article ID: 1003-1057(2015)8-501-13

1. Introduction

Nanomicelle delivery systems, which are usually self-assembled by biocompatible amphiphilic materials in aqueous medium, are more promising for hydrophobic anticancer drugs delivery^[1,2]. The hydrophilic surface of micelles provides particle stabilization in aqueous solution and prevents rapid uptake by the reticuloendothelial system (RES)^[3-5]. Moreover, the limited particle size of 5–100 nm in diameter can enhance micellar accumulation in tumors through the enhanced permeability and retention (EPR) effect^[6]. Currently, some micelle-based delivery systems have been employed in clinical trials, including NK105 (paclitaxel-loaded polyethylene glycol-(L-aspartic acid) micelles), NK012 (SN-38, ethylhydroxycamptothecin-conjugated polyethylene glycol-poly

(L-glutamic acid) micelles)^[7], NC-6004 (cisplatin-loaded polyethylene glycol-poly (L-benzylglutamic acid) micelles)^[8], and SP1049C (doxorubicin-loaded Pluronic micelles)^[9]. Therefore, nanomicelle delivery systems are worthy of further research to promote chemotherapy evolution.

However, nanomicelle delivery systems still encounter many problems, such as how to increase the selectivity to tumor cells and enhance targeting efficiency at the tumor sites^[10]. Many reports suggested that specific targeting ligand-modified micelles are effective to enhance drug accumulation in tumors. The commonly used ligands, including arginine-glycine-aspartic acid tripeptide (RGD)^[11], folate^[12], transferrin^[13] and epidermal growth factor (EGF)^[14], can recognize the unique receptors overexpressed on different cancer cells.

Somatostatin receptors (SSTRs), especially SSTR subtype 2 (SSTR2), are found expressed at relatively higher levels in many tumor cells compared with normal tissues. For example, it has been proved that MCF-7 cells overexpress SSTR2 in comparison with Chinese hamster ovary cells^[15]. This result indicated that

Received: 2015-05-03; Revised: 2015-05-15; Accepted: 2015-05-20.
Foundation items: National Basic Research Program of China (973 Program, Grant No. 2013CB932501), NSFC projects (Grant No. 81273455 and 81473158), and Programs from Ministry of Education (Grant No. NCET-11-0014 and BMU20110263).

*Corresponding author. Tel.: 86-10-82805932;

E-mail: wang-jc@bjmu.edu.cn

<http://dx.doi.org/10.5246/jcps.2015.08.064>

SSTR2 is a potential target spot for tumor diagnosis and treatment. In fact, ^{111}In -DTPA-octreotide was approved by the FDA in June 1994 for the diagnosis of various neuroendocrine tumors^[16]. In addition, previous studies assessed antitumor agents conjugated with somatostatin analogues, such as DOX^[17,18], paclitaxel^[19] and camptothecin^[20,21], and these results presented good potential of somatostatin analogues in drug delivery.

As an octapeptide analogue of endogenous somatostatin, vapreotide (RC-160) has high affinity for SSTR2^[22,23]. Some studies have demonstrated the effects of $^{99\text{m}}\text{Tc}$ -RC-160 and ^{131}I -RC-160 in tumor diagnosis and therapy^[24]. However, it is rarely reported that vapreotide is used as a targeting ligand modified on nanocarriers for drug delivery. Importantly, previous studies have reported that the disulfide bridge and a stretch of key amino acids (Phe-Trp-Lys-Val) in the structure of vapreotide are critical for binding with SSTR2^[25]. In order to avoid $\epsilon\text{-NH}_2$ of lysine (Lys) directly connected with carriers which may reduce the binding activity of vapreotide with SSTR2, selective conjugation between carriers and $\alpha\text{-NH}_2$ of exocyclic D-phenylalanine (D-Phe) in vapreotide is necessary^[26]. Compared with our previous studies on octreotide (a somatostatin analogue) modified drug delivery system^[15,27], this work supposed the possibility of Lys- NH_2 protection on vapreotide to prevent the loss of biological activity.

With this hypothesis, we designed vapreotide-modified micelle delivery system to deliver paclitaxel for the treatment of SSTR2-overexpressing tumors in this study. Moreover, $\alpha\text{-NH}_2$ of exocyclic D-Phe on the Lys-protected vapreotide (Lys-DDE) was specially conjugated with PEG₂₀₀₀-DSPE through NHS activated group, whereafter, the protective group DDE was removed by deprotection method, thereby the final DSPE-PEG-VAP (Lys- NH_2) was obtained. Vapreotide-modified Paclitaxel (PTX)-loaded targeted micelles (VAP-M-PTX) were assembled by DSPE-PEG₂₀₀₀-VAP (Lys- NH_2), PEG₂₀₀₀-DSPE, D- α -tocopheryl polyethylene glycol 1000 succinate (TPGS) and PTX as previously described^[28]. At the same time, PTX-loaded non-targeted micelles (M-PTX) consisting of PEG₂₀₀₀-DSPE, TPGS and PTX were used as the control. To prove the targeting effect, we investigated cellular uptake and cytotoxicity of vapreotide-modified

micelles on MCF-7 cells in vitro. In addition, we also evaluated the antitumor efficacy of VAP-M-PTX in vivo and the drug distribution in tumor tissues in nude mice xenografted MCF-7 tumors.

2. Materials and methods

2.1. Materials

Lys-protected Vapreotide (Lys-DDE) (Mw 1295.6, purity>95%) was synthesized by GL BioChem Ltd. (Shanghai, China). Paclitaxel was purchased from Knowshine BioChem Ltd. (Shanghai, China), and 1,2-Distearoyl-sn-glycero-3-phosphoethanolamine [methoxy (polyethylene glycol)-2000] (DSPE-PEG) and *N*-hydroxysuccinimidyl-PEG₂₀₀₀-DSPE (NHS-PEG-DSPE) were obtained from NOF Co. (Tokyo, Japan). Taxol[®] containing 30 mg paclitaxel in 5 mL mixture of Cremophor EL–ethanol (1:1, v/v) was commercially available from the local hospital in Beijing (Bristol-Mayer Squibb Co., Princeton, NJ, USA). Near-infrared lipophilic carbocyanine dye 1,1'-diiodododecyl-3,3',3'-tetramethyl indotricarbocyanine iodide (DiR) was supplied from Biotium, Inc. (Hayward, CA, USA). Hoechst 33258 and coumarin 6 (Cou, purity>99%) were provided by Molecular Probes Inc. (Eugene, OR, USA). D- α -Tocopheryl polyethylene glycol 1000 succinate (TPGS), sulforhodamine B (SRB) and Tris-base were purchased from Sigma-Aldrich (St. Louis, MO, USA). Cell culture medium RPMI-1640, penicillin-streptomycin, fetal bovine serum and trypsin were obtained from M&C Gene Technology (Beijing, China). All other reagents were of analytical grade.

Human breast cancer (MCF-7) cells were obtained from the Institute of Basic Medical Science, Chinese Academy of Medical Sciences (Beijing, China). Cells were maintained in RPMI-1640 medium supplemented with 10% fetal bovine serum, 100 U/mL penicillin and 100 $\mu\text{g/mL}$ streptomycin, at 37 °C in 5% CO₂ atmosphere.

2.2. Synthesis of DSPE-PEG-VAP

Vapreotide conjugated with PEG-DSPE was obtained as following methods. Briefly, Lys-protected vapreotide (Lys-DDE) and NHS-PEG-DSPE (1/2, Mol/Mol) were

adjusted to 8–9 with triethylamine, the reaction mixture was further stirred at room temperature for 24 h. As an indicator of the reaction process, the free vapreotide concentration in reaction mixture was monitored by RP-HPLC analysis (Shimadzu, LC-10AT, Japan). The diluted sample solution was eluted in a C₁₈ column with a mobile phase containing acetonitrile–water (45:55, v/v) with 0.1% trifluoroacetic acid at a flow rate of 1 mL/min, and it was further detected by a Ultra-Violet detector at a wavelength of 220 nm. After reaction for 24 h, the deprotection reagents (final concentrations: 327 mM for NH₂OH·HCl and 245.1 mM for imidazole) were added in this reaction mixture according to the method as previously described^[29]. The reaction was continuously maintained at room temperature for 2 h, and the reaction product was monitored by Matrix-Assisted Laser Desorption/Ionization Time of Flight Mass Spectrometry (MALDI-TOF-MS, AXIMA-CFR Plus, Shimadzu, Japan) using a matrix consisting of 10 mg/mL α -cyano-cinnamic acid in a solution of acetonitrile–water (1:1, v/v) with 0.1% trifluoroacetic acid. After the reaction was terminated, the products were dialyzed (molecular weight cutoff = 3500 Da) against deionized water for 48 h to remove redundant reagents and solvents. The solution in dialysis bag was lyophilized and stored at –20 °C prior to further analysis. Successful conjugation of DSPE-PEG-VAP (Lys-NH₂) was confirmed by MALDI-TOF-MS.

2.3. Preparation of PTX-loaded micelles

All the micelles were prepared using a thin-film hydration method^[30]. In preparation of targeted VAP-M-PTX micelles, a mixture of 10 mg DSPE-PEG-VAP (Lys-NH₂), 23.35 mg PEG-DSPE, 16.67 mg TPGS and 2 mg PTX were dissolved in 10 mL acetonitrile in a round-bottom flask, which was connected to an RE52 rotary evaporator (Shanghai Yarong Biochemistry Instrument Company, China) and a water bath (B-260) at 37 °C. In order to form a homogeneous thin film on the flask wall, acetonitrile was evaporated by vacuum. The dry thin film was incubated at 60 °C for 10 min to remove traces of acetonitrile. Subsequently, 2 mL saline solution was added to hydrate the film, and the resulting

hydration mixture was incubated at 60 °C for 20 min. Free PTX was separated by filtration of the micelles suspension through a 0.22- μ m poly (ether sulfone) membrane (MEMBRANA Co., Germany). The final VAP-M-PTX was obtained with a concentration of 1 mg PTX/mL and 25 mg materials/mL. For M-PTX, the preparation procedure was same as above-mentioned for VAP-M-PTX except that the equivalent molar of DSPE-PEG-VAP (Lys-NH₂) was replaced by PEG-DSPE. Moreover, fluorescent probes coumarin 6 (Cou)- or DiR-loaded polymeric micelles (VAP-M-Cou and M-Cou or VAP-M-DiR and M-DiR) were prepared using the same method except that PTX was replaced by Cou or DiR.

2.4. Characterization of PTX-loaded micelles

The particle size, polydispersity index (PDI) and zeta potential of various micelles were determined by dynamic light scattering (DLS) using a Malvern Zetasizer Nano ZS (Malvern, U.K.). The morphologies of micelles were observed by transmission electron microscopy (TEM, JEOL, JEM-1400, Japan) after micelles were negatively stained with 1% phosphotungstic acid solution. The encapsulation efficiency of PTX in micelles was measured by RP-HPLC analysis. The micelles were destroyed by methanol, and the analysis was performed on ODS column (phenomenex[®] C₁₈, 5 μ m, 250 mm×4.6 mm). The mobile phase consisted of methanol–acetonitrile–water (40:30:30, v/v/v), and UV detection was monitored at a wavelength of 227 nm. The encapsulation efficiency was then calculated as the drug loaded in the micelles divided by total drug used.

2.5. Drug release in vitro

The release of PTX from PTX-loaded micelles in vitro was performed in the release medium containing 0.5% Tween-80 at 37 °C. The solutions of M-PTX, VAP-M-PTX and Taxol[®] equivalent to 0.06 mg PTX were diluted to 1 mL with the release medium in dialysis bags using a cutoff mass ranging from 12 000 to 14 000 Da. Then the dialysis bags were maintained in 40 mL of release medium containing 0.5% Tween-80 at 37 °C for 48 h and stirred at 100 r/min. At predetermined time points, aliquots (200 μ L) were taken from the beaker,

and an equal volume of fresh medium was supplemented. The concentrations of PTX in samples were determined by RP-HPLC after appropriate dilution with methanol.

2.6. Hemolysis evaluation

Briefly, fresh blood was collected from a Sprague-Dawley rat (purchased from Vital Laboratory Animal, Beijing, China) by cardiac puncture, and collected samples were washed with normal saline and centrifuged at 1500 r/min for 15 min. The supernatant was removed, and the precipitate was washed using normal saline for two times. Subsequently, the red blood cells (RBCs) were diluted to 2% of suspension with normal saline. RBC suspension (500 μ L) was added to 500 μ L Taxol[®], M-PTX and VAP-M-PTX samples with a concentration of 0.01 to 1 mg PTX/mL, respectively. After incubation at 37 °C for 1 h, the mixture was centrifuged at 2000 r/min for 10 min to remove non-lysed RBCs. The supernatants (200 μ L) were collected to a 96-well plate and detected at a wavelength of 540 nm using a microplate reader (Multiskan MK3, Thermo, Waltham, MA, USA). To obtain 0% and 100% hemolysis, 500 μ L 2% RBC suspension was added to 500 μ L normal saline and 500 μ L distilled water, respectively. The hemolytic rate was calculated by the equation as follows: $\text{hemolysis\%} = (A_{\text{sample}} - A_{0\%}) / (A_{100\%} - A_{0\%}) \times 100\%$. A_{sample} , $A_{0\%}$ and $A_{100\%}$ represent the absorbance of test samples, 0% hemolysis and 100% hemolysis, respectively. The experiment was performed in triplicate.

2.7. Cellular uptake

In cellular uptake studies, flow cytometry was used to quantify intracellular fluorescence intensity. As a fluorescence probe, coumarin 6 was loaded in targeted micelles (VAP-M-Cou) and non-targeted micelles (M-Cou). MCF-7 cells were seeded in 6-well plates at a density of approximately 3.5×10^5 cells/well and incubated at 37 °C 24 h for cell attachment. Then the medium was replaced by 2 mL/well serum-free medium containing M-Cou or VAP-M-Cou (the concentration of Cou was 200 ng/well). After incubation for 3 h, the cells were trypsinized and collected by centrifugation, washed for three times by cold PBS and examined by flow

cytometry using FACS instrument (Becton Dickinson, San Jose, CA). Intracellular fluorescence intensity of coumarin-6 was excited with an argon laser (488 nm) and detected at a wavelength of 560 nm. Files were analyzed by FACStation software program.

For confocal microscopy analysis, MCF-7 cells were cultured in glass-bottomed dishes and maintained at 37 °C for 24 h. As same as flow cytometry analysis, the old cultural medium was replaced by 2 mL/well of the serum-free medium containing M-Cou or VAP-M-Cou, and the dishes were incubated at 37 °C for another 3 h. Subsequently, the dishes were washed three times by cold PBS and fixed with 4% paraformaldehyde in PBS. After fixation, the cells were stained with Hoechst 33258 for 15 min. Finally, the samples were examined by a Leica SP5 confocal microscope (TCS SP5, Leica, Heidelberg, Germany). Coumarin 6 and Hoechst 33258 were excited at a wavelength of 488 nm and 352 nm, respectively. The emission wavelengths of coumarin 6 and Hoechst 33258 were 560 nm and 460 nm, respectively.

2.8. In vitro cytotoxicity study

The antiproliferation efficacy was evaluated using sulforhodamine B (SRB) assay^[31]. Briefly, MCF-7 cells were seeded at a density of 5000 cells/well in 96-well plates and cultured at 37 °C. After proliferation for 24 h, cells were incubated at 37 °C for another 48 h with 200 μ L of M-PTX, VAP-M-PTX and Taxol[®] (containing 1, 2, 4, 8, 16, 32, 64, 128 nM of PTX) in RPMI 1640 medium. Subsequently, the cells were processed by SRB assay as above-mentioned. Each sample was performed in triplicate. The dose-response curve was generated, and the half maximal inhibitory concentration (IC_{50}) of each formulation was calculated accordingly.

2.9. In vivo tissue distribution of DiR-loaded micelles

In order to observe in vivo tissue distribution of nanomicelles after intravenous injection, fluorescence dye DiR was loaded in micelles as a probe, and non-invasive imaging system was utilized^[32].

Approximately 3.0×10^6 MCF-7 cells were subcutaneously inoculated in the right armpits of nude mice. When the tumor reached 150 mm³, M-DiR and VAP-M-DiR

equivalent to 1 μg of DiR (50 $\mu\text{g}/\text{kg}$) in 200 μL saline were injected to the mice via the tail vein, respectively. Subsequently, isoflurane was used to anaesthetize those nude mice via an air anesthesia apparatus (Matrx VIP 3000, Midmark, NY, USA). In vivo imaging experiments were performed at 12, 24 and 48 h post-injection using a KODAK in vivo imaging system (Kodak FX Pro, Carestream Health, NY, USA). After mice were sacrificed at 48 h, tumors and major organs, including heart, liver, spleen, lung and kidney, were excised and separately imaged with the same system. The results were analyzed using the image station IS2000MM.

2.10. In vivo antitumor efficacy

In vivo antitumor efficacies of various micelles were evaluated on MCF-7 tumor-bearing nude mice. Female BALB/c nude mice were purchased from Vital Laboratory Animal Center (Beijing, China) at 6 weeks of age (initially weighing 18–20 g). All care and handling of animals were performed with the approval of Institutional Animal Care and Use Committee at Peking University Health Science Center. In this study, 3.0×10^6 MCF-7 cells were subcutaneously inoculated in the right armpits of nude mice as above-mentioned. On the 7th day, the MCF-7 tumor-bearing mice were randomly assigned to four groups ($n = 6$) as follows: group 1 for saline solution, group 2 for Taxol[®] formulation (10 mg PTX/kg), group 3 for M-PTX formulation (10 mg PTX/kg), and group 4 for VAP-M-PTX formulation (10 mg PTX/kg). Mice were administered with formulations through tail vein at the day of 7, 10, 12 and 14. Tumor size were measured by a Vernier caliper, and the tumor volume was calculated with the formula as follows: Tumor volume = $(\text{length} \times \text{width}^2/2)^{[33]}$. On the 16th day, tumor-bearing mice were sacrificed, and the tumors were excised for further observation by KODAK imaging system.

2.11. Statistical analysis

All the experiments were performed at least three times. Results were expressed as mean \pm standard deviation (SD) unless particularly outlined. All data were calculated by Student's *t*-test or ANOVA test. $P < 0.05$ was considered as statistically significant.

3. Results and discussion

3.1. Synthesis of DSPE-PEG-VAP

Figure 1 shows the synthesis scheme of DSPE-PEG-VAP (Lys-NH₂). The Lys-protected Vapreotide (Lys-DDE) was conjugated with NHS-PEG-DSPE through the NHS active group, and the reaction process was monitored by RP-HPLC (Fig. 2A). After reaction for 24 h, no free vapreotide was detected in the reaction mixture, indicating that most of peptides were connected with NHS-PEG-DSPE. Figure 2B shows that the successful conjugation of DSPE-PEG-VAP (Lys-DDE) was further confirmed by the molecular weight (m/z value 4200–4300) determined by MALDI-TOF-MS method, which was consistent with the theoretical value. Furthermore, the final product (DSPE-PEG-VAP (Lys-NH₂)) was obtained from deprotection of DSPE-PEG-VAP (Lys-DDE), and its molecular weight was verified by MALDI-TOF Mass Spectrum. Figure 2C exhibits that the molecular weight of DSPE-PEG-VAP (Lys-NH₂) determined by MALDI-TOF-MS was about 4000–4100 (m/z value). The difference of m/z value between DSPE-PEG-VAP (Lys-DDE) and DSPE-PEG-VAP (Lys-NH₂) was approximately 200, which was equal to the molecular weight of DDE protection group. Therefore, we concluded that the synthesis of DSPE-PEG-VAP (Lys-NH₂) was successful.

Previous study has reported that the disulfide bridge and a stretch of key amino acids (Phe-Trp-Lys-Val) in the structure of vapreotide are critical for binding with SSTR2^[25]. In order to avoid reducing the binding activity of vapreotide with SSTR2 owing to DSPE-PEG-NHS directly connected with ϵ -NH₂ of lysine (Lys), selective conjugation is necessary between DSPE-PEG-NHS and α -NH₂ of exocyclic D-Phe on vapreotide^[26]. Here, we selected a commercial Fmoc-Lys(DDE)-OH as a protected lysine used for synthesis of Lys-protected vapreotide (Lys-DDE), and then the α -NH₂ of exocyclic D-Phe on vapreotide was exclusive to conjugate with DSPE-PEG-NHS. After that, the DDE amine protecting group on the DSPE-PEG-VAP (Lys-DDE) was further deprotected by a mixed reagents of NH₂OH-HCl and imidazole^[29]. In this work, we hypothesized that the protection of Lys-NH₂ on vapreotide could be beneficial to prevent the loss of biological activity.

3.2. Preparation and characterization of drug-loaded micelles

Figures 3A₁ and 3B₁ exhibit typical schematic illustration of M-PTX and VAP-M-PTX. Typical morphologies of M-PTX micelles (Fig. 3A₂) and VAP-M-PTX micelles (Fig. 3B₂) were observed by transmission electron microscope. The size distribution and zeta potential of M-PTX micelles (Fig. 3C₁ and 3C₂) and VAP-M-PTX micelles (Fig. 3C₃ and 3C₄) were determined by dynamic light scattering method. Table 1 summarizes the data of average sizes, polydispersity indexes (PDI), zeta potential values, encapsulation efficiencies and loading capacities of various micelles. In comparison of M-PTX and VAP-M-PTX micelles, the modification of

vapreotide did not significantly affect the physical-chemical properties of micelles. Moreover, different encapsulated drugs (PTX, DiR or Cou) did not change the physical-chemical properties of micelles, including hydrodynamic diameter (about 30 nm), PDI (around 0.25) and encapsulation efficiency (more than 90%), suggesting that it was feasible to trace the fate of drug-loaded micelles in vitro or in vivo using DiR and Cou as fluorescence probes for the next experiments^[34]. On the other hand, all the prepared micelles exhibited weak negative surface charge (−0.4 mV~ −5.4 mV) and uniform size distribution (24–36 nm) (Table 1), suggesting that the micelles could be favorable to decrease the uptake by nonspecific organs and provide the better targeting effect in vivo^[35].

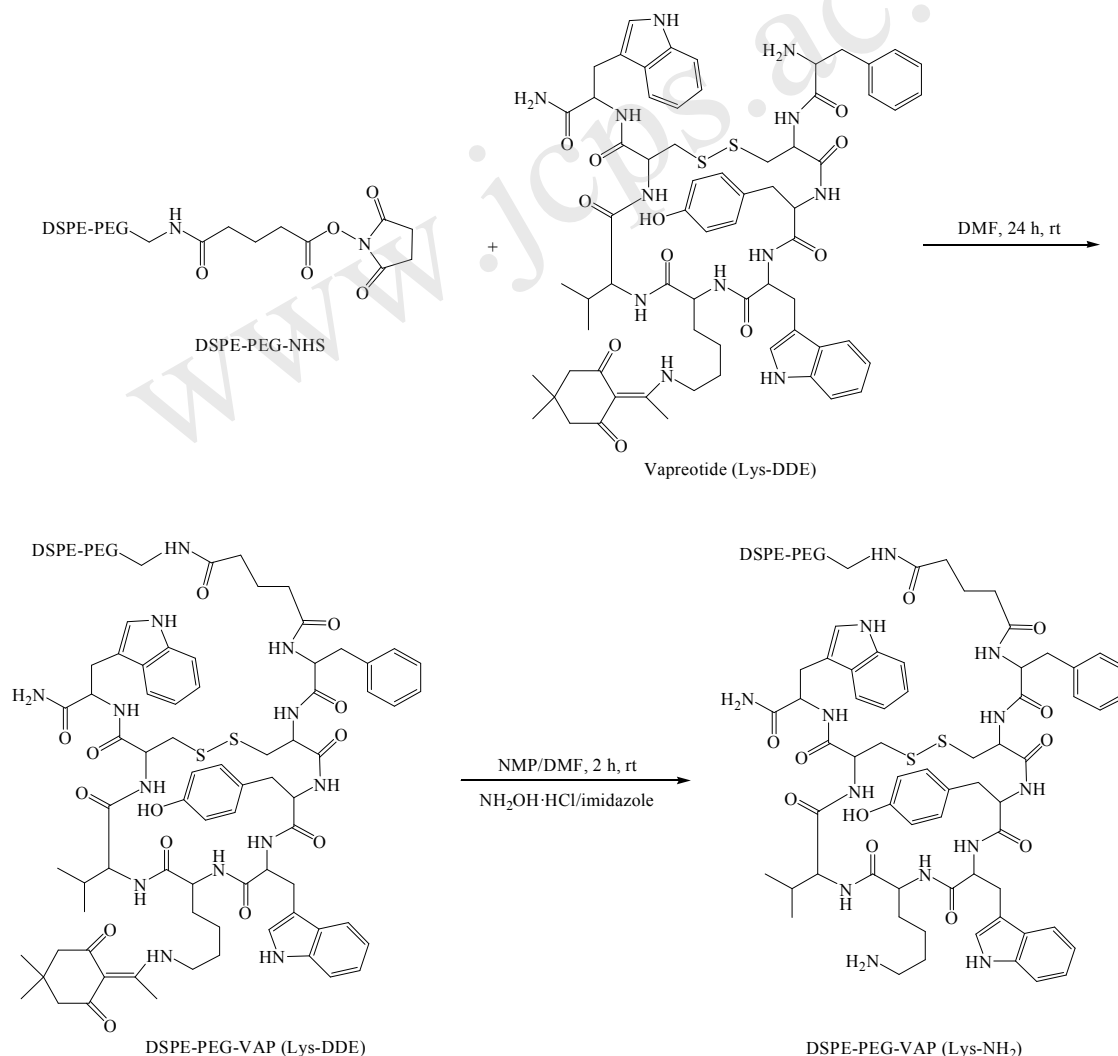
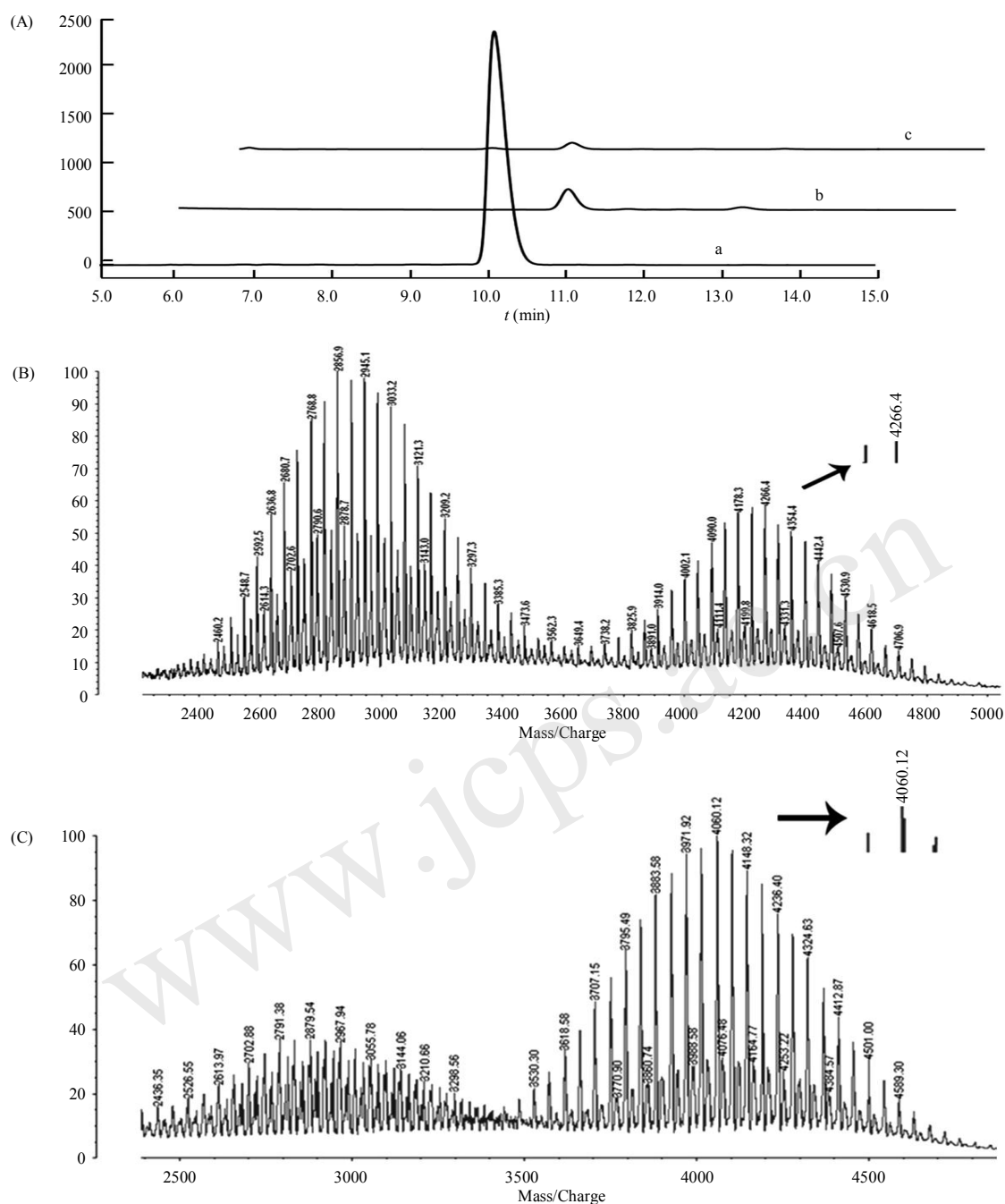


Figure 1. Synthetic procedure of DSPE-PEG-VAP (Lys-NH₂).



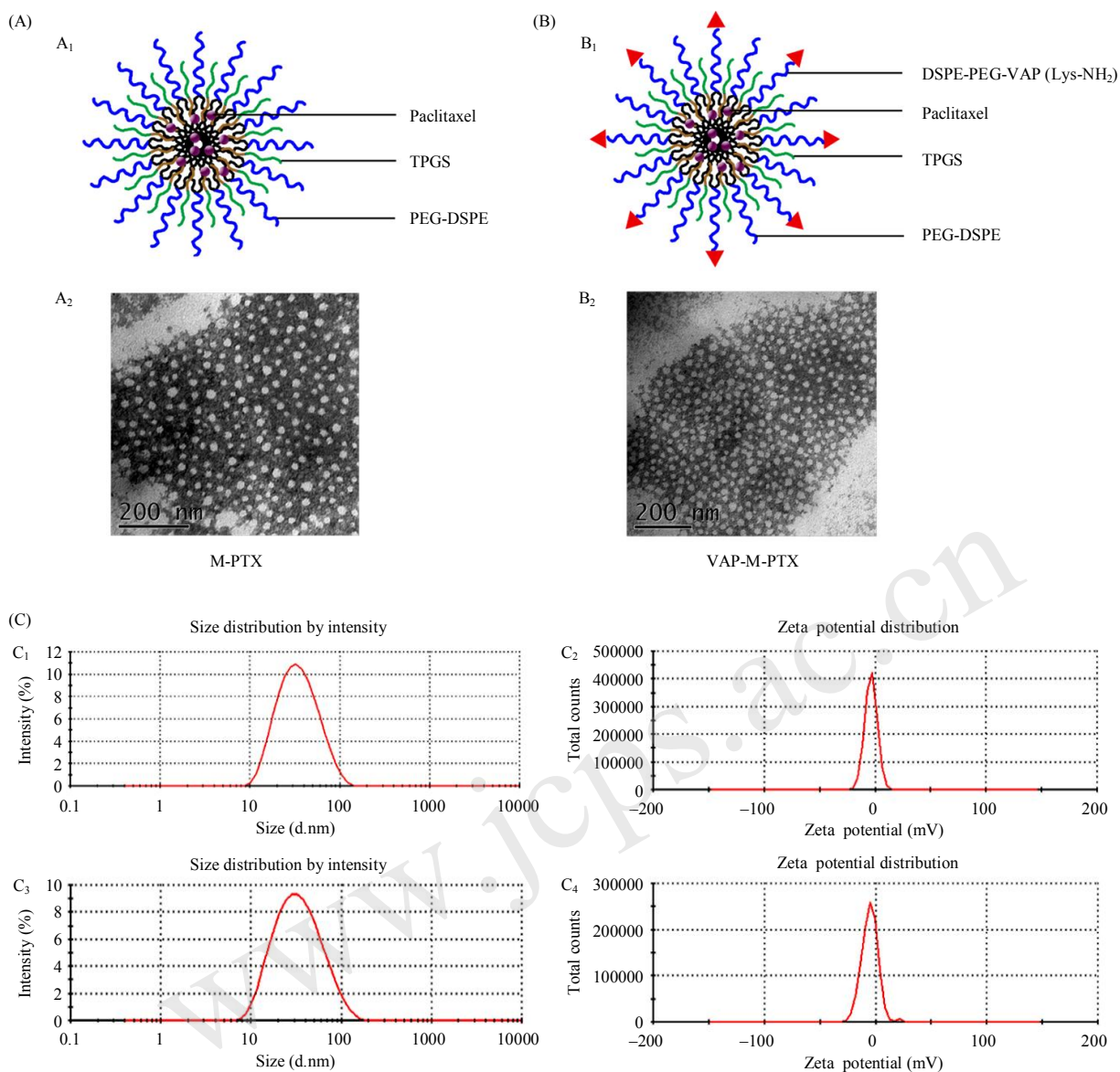


Figure 3. Schematic illustration of M-PTX micelles (A₁) and VAP-M-PTX micelles (B₁). Typical TEM images of M-PTX micelles (A₂) and VAP-M-PTX micelles (B₂) stained with 1% Phosphotungstic acid. Particle size and zeta potential of M-PTX micelles (C₁, C₂) and VAP-M-PTX micelles (C₃, C₄).

3.3. Drug release in vitro

Figure 4A shows that no significant difference in drug release was observed at each time point between M-PTX micelles and VAP-M-PTX micelles. At 48 h, the maximum cumulative release of PTX from M-PTX, VAP-M-PTX and Taxol[®] were 92.26%±3.82%, 96.58%±1.88% and 93.14%±2.02%, respectively. These results indicated little influence of the vaporeotide modification on PTX release. Considering a solubilizer (0.5% Tween-80) added in the release medium, the actual drug release was rather slow. Moreover, no significant leakage of PTX from

micelles with or without vaporeotide modification was found within 48 h when stored at 4 °C.

3.4. Hemolysis evaluation

Figure 4B shows that the hemolysis induced by Taxol[®] was continuously increased along with the increase of PTX concentration from 0.1 mg/mL to 1 mg/mL. However, M-PTX and VAP-M-PTX exhibited little hemolysis activity at a concentration of even up to 1 mg/mL. At the concentration of 1 mg/mL, the hemolysis of Taxol[®], M-PTX and VAP-M-PTX was 49.9%, 2.3%

and 2.1%, respectively. This indicated that M-PTX and VAP-M-PTX had little hemolytic potential and might be safe for i.v. administration relative to Taxol®. The high hemolysis of Taxol® among all tested formulations might be resulted from the toxicity of Cremophor EL and ethanol involved.

3.5. Cellular uptake

In MCF-7 cells, we detected a significantly higher fluorescence intensity (1.5-fold) by flow cytometry after incubation of coumarin-6 for 3 h in loaded targeted micelles (VAP-M-Cou) compared with non-targeted

micelles (M-Cou) (Fig. 5A and 5B), and similar observation was found from confocal microscopy (Fig. 5C). Therefore, we doubtless believed that the vapreotide modification could significantly enhance cell uptake of micelles in MCF-7 cells. It has been proved that ligand-modified nanoparticles can promote uptake by cells through a receptor-mediated endocytosis pathway because of the special interaction between ligand and receptor^[36,37]. Based on these findings, it suggested that the targeted VAP-M-Cou micelles could achieve a better targeting efficiency for delivering drug to the SSTR2-overexpression tumor in vivo after intravenous administration.

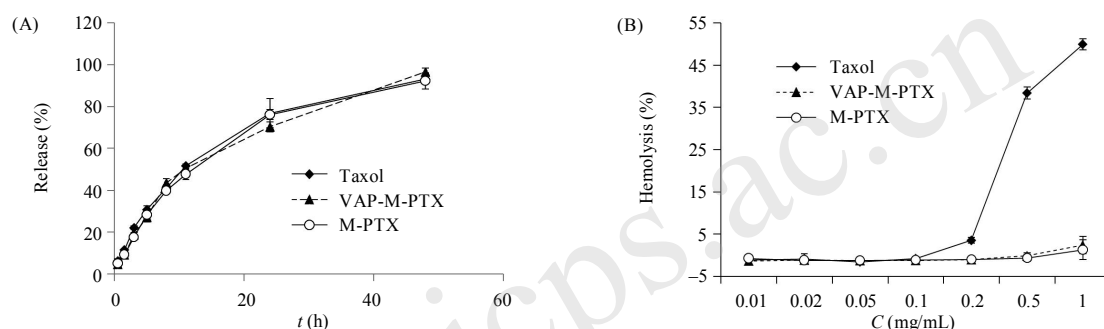


Figure 4. (A) In vitro release of PTX from M-PTX and VAP-M-PTX. (B) Hemolysis evaluation of M-PTX, VAP-M-PTX and Taxol with a series of concentrations of paclitaxel.

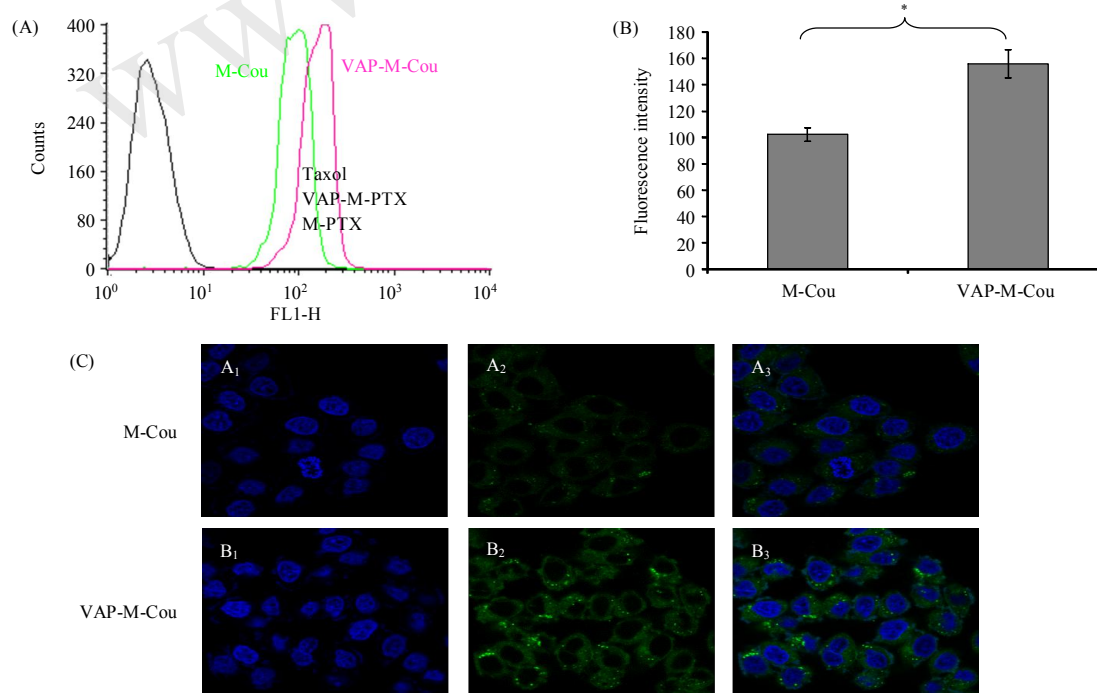


Figure 5. Fluorescence intensity of coumarin-6 in MCF-7 cells after incubation with M-Cou (A) and VAP-M-Cou (B) determined by flow cytometry (* $P < 0.01$). (C) Confocal microscopy images of MCF-7 incubated with M-Cou (A₁A₂A₃) and VAP-M-Cou (B₁B₂B₃) for 3 h at 37 °C. The concentration of Coumarin 6 was 200 ng/mL for all formulations. Green represents fluorescence of coumarin 6. Blue represents fluorescence of Hoechst 33258, which shows the nuclear.

3.6. In vitro cytotoxicity

Figure 6 shows that the corresponding IC_{50} values of M-PTX, VAP-M-PTX and Taxol[®] on MCF-7 cells were (23.11 ± 1.83) nM, (19.14 ± 0.23) nM and (14.80 ± 0.53) nM respectively. Obviously, the anti-proliferation ability was in an order as follows: Taxol[®] > VAP-M-PTX > M-PTX ($P < 0.05$). The lower IC_{50} value of VAP-M-PTX compared with M-PTX indicated that vaporeotide modification might be effective on increasing the toxicity of PTX-loaded micelles against MCF-7 cancer cells, which was likely resulted from the enhanced cellular uptake through SSTR2-mediated endocytosis as proved by the above-mentioned results of flow cytometry and confocal microscopy studies. Therefore, we believed that the modification of vaporeotide on the surface of nanocarrier played an important role in the cytotoxicity enhancement of paclitaxel on the SSTR-overexpressed tumor cells.

3.7. In vivo distribution of DiR-loaded micelles

The Kodak in vivo imaging system was adopted to visualize tissue distribution of DiR-loaded micelles at different time points (12, 24 and 48 h) after intravenous injection. Figure 7A shows that the tumor accumulation of VAP-M-DiR was higher than that of M-DiR at each time point. Even at 48 h, a higher fluorescence signal in tumor was detected in the mice administered with VAP-M-DiR micelles. However, a weaker fluorescence was found in M-DiR micelles. The ex vivo imaging of tumors and organs excised from the mice at 48 h further proved that more VAP-M-DiR was accumulated and retained in tumor tissues than compared with M-DiR (Fig. 7B). These results indicated that vaporeotide modification could effectively increase the accumulation of micelles in tumors through active targeting pathway more than the EPR effect.

Moreover, except for liver tissue, no detectable fluorescence found was detected in heart, spleen, lung and kidney. A significant fluorescence accumulation in liver after intravenous injection of either VAP-M-PTX or M-PTX micelles suggested that the micellar nanoparticles were still entrapped by RES during circulation, especially in liver, even though PEGlyted micelles exhibited the

ability of avoiding rapid uptake by RES to a certain degree. Moreover, it should be noted that carbocyanine dye (DiR) is prone to be taken up exclusively by hepatic parenchymal cell as soon as it is released from micelles because of its lipophilic characteristics^[38].

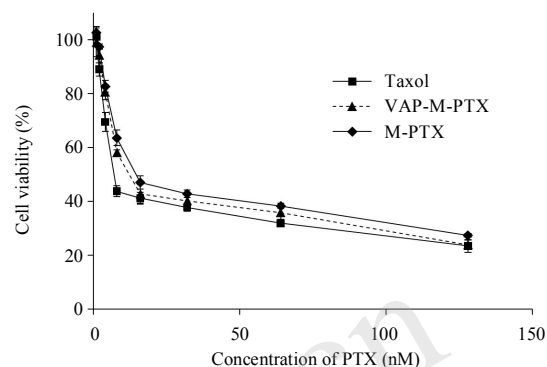


Figure 6. Cytotoxicity of M-PTX, VAP-M-PTX and Taxol formulations on MCF-7 cells.

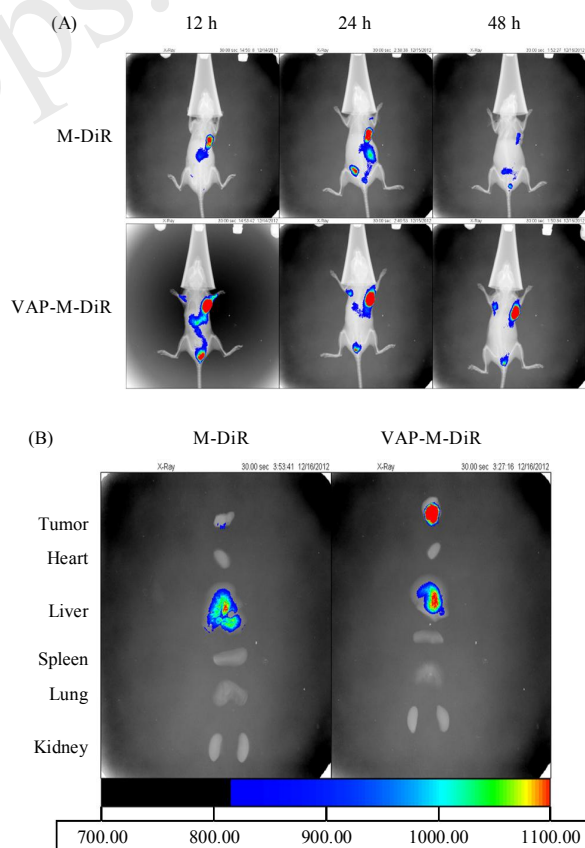


Figure 7. (A) In vivo tissue distribution of M-DiR and VAP-M-DiR in nude mice xenografted MCF-7 tumors at 12 h, 24 h and 48 h after intravenous injection (DiR, $\lambda_{ex} = 748$ nm, $\lambda_{em} = 780$ nm). (B) The ex vivo imaging of DiR accumulation in heart, liver, spleen, lung, kidney and tumor at 48 h.

3.8. In vivo antitumor efficacy

To investigate the antitumor efficacy of PTX formulations, female BALB/c nude mice bearing MCF-7 xenograft were randomly divided into four groups ($n = 6$) and treated with different formulations by intravenous injection. Figure 8A shows that on the 15th day, tumor growth was significantly inhibited in the PTX-treated groups ($P < 0.01$) compared with the saline group. The mean tumor volumes corresponding to VAP-M-PTX, Taxol[®], M-PTX and saline groups on 15th day were $(157.13 \pm 42.0) \text{ mm}^3$, $(302.37 \pm 144.53) \text{ mm}^3$, $(454.51 \pm 141.38) \text{ mm}^3$ and $(1292.41 \pm 287.87) \text{ mm}^3$, respectively. The corresponding tumor growth inhibition efficiencies of VAP-M-PTX, Taxol[®] and M-PTX formulations were 87.84%, 76.60% and 64.83%, respectively. Figure 8B exhibits the images of excised tumors corresponding to the treatments of saline solution, Taxol[®], M-PTX and VAP-M-PTX.

It indicated that VAP-M-PTX micelles showed the strongest inhibition effect on tumor growth among all formulations ($P < 0.05$ vs. Taxol[®], $P < 0.01$ vs. M-PTX) tested in MCF-7 tumor-bearing mice. Compared with M-PTX, the higher antitumor efficacy of VAP-M-PTX might be resulted from receptor-mediated tumor targeting effects based on the modification of vapreotide on the surface of micelles. As reported previously, passive targeting micelles (non-targeted micelles in this study) accumulated in tumor tissue are mainly based on the EPR effect^[39], whereas the accumulation of active targeting nanocarriers in tumor cells is mainly based on the receptor-mediated endocytosis and ERP effect^[40]. Therefore, we concluded that the active targeting strategy based on VAP modification on the surface of micelles could improve the therapeutic efficacy of antitumor drugs.

4. Conclusions

In this study, we used vapreotide as a targeting ligand modified on the nanomicelle due to its high affinity to SSTR2 overexpressed MCF-7 breast cancer cells. Compared with those non-targeted formulations,

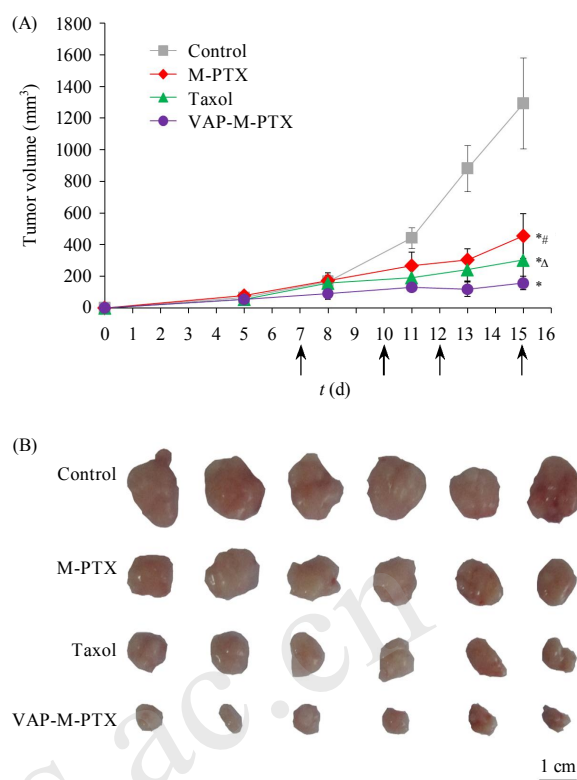


Figure 8. (A) Tumor growth inhibition curves of saline solution, Taxol, M-PTX and VAP-M-PTX in female BALB/c nude mice xenografted MCF-7 tumors after given four doses (each dose of 10 mg of PTX/kg) at 7, 10, 12, 14 d after inoculation (as the arrows indicated). Data represent mean \pm SD ($n = 6$). * $P < 0.01$ vs control group at the 15th day; # $P < 0.01$, $^{\Delta}P < 0.05$ vs VAP-M-PTX group at 15th day. (B) Photos of excised tumors corresponding to the treatments of saline solution, Taxol, M-PTX and VAP-M-PTX.

the prepared VAP-M-PTX micelles exhibited a higher antitumor efficacy and a higher drug accumulation in BALB/c nude mice xenografted MCF-7 tumors after intravenous injection. Therefore, we believed that vapreotide-modified nanomicelle could be a promising and potential targeted delivery system for delivering anticancer drugs to the tumors overexpressing somatostatin receptors.

Acknowledgements

This work was financially supported by National Basic Research Program of China (973 Program, Grant No. 2013CB932501), NSFC Projects (Grant No. 81273455 and 81473158), and Programs from Ministry of Education (Grant No. NCET-11-0014 and BMU20110263).

References

- [1] Cai, S.; Vijayan, K.; Cheng, D.; Lima, E.M.; Discher, D.E. *Pharm. Res.* **2007**, *24*, 2099–2109.
- [2] Lin, J.; Zhang, S.; Chen, T.; Lin, S.; Jin, H. *Int. J. Pharm.* **2007**, *336*, 49–57.
- [3] Gaur, U.; Sahoo, S.K.; De, T.K.; Ghosh, P.C.; Maitra, A.; Ghosh, P.K. *Int. J. Pharm.* **2000**, *202*, 1–10.
- [4] Kataoka, K.; Harada, A.; Nagasaki, Y. *Adv. Drug Deliv. Rev.* **2001**, *47*, 113–131.
- [5] Savic, R.; Luo, L.; Eisenberg, A.; Maysinger, D. *Science* **2003**, *300*, 615–618.
- [6] Matsumura, Y.; Maeda, H. *Cancer Res.* **1986**, *46*, 6387–6392.
- [7] Matsumura, Y. *Adv. Drug Deliv. Rev.* **2008**, *60*, 899–914.
- [8] Plummer, R.; Wilson, R.H.; Calvert, H.; Boddy, A.V.; Griffin, M.; Sludden, J.; Tilby, M.J.; Eatock, M.; Pearson, D.G.; Ottley, C.J.; Matsumura, Y.; Kataoka, K.; Nishiya, T. *Br. J. Cancer* **2011**, *104*, 593–598.
- [9] Danson, S.; Ferry, D.; Alakhov, V.; Margison, J.; Kerr, D.; Jowle, D.; Brampton, M.; Halbert, G.; Ranson, M. *Br. J. Cancer* **2004**, *90*, 2085–2091.
- [10] Mahmud, A.; Xiong, X.B.; Aliabadi, H.M.; Lavasanifar, A. *J. Drug Target.* **2007**, *15*, 553–584.
- [11] Cai, L.L.; Liu, P.; Li, X.; Huang, X.; Ye, Y.Q.; Chen, F.Y.; Yuan, H.; Hu, F.Q.; Du, Y.Z. *Int. J. Nanomedicine* **2011**, *6*, 3499–3508.
- [12] Niu, R.; Zhao, P.; Wang, H.; Yu, M.; Cao, S.; Zhang, F.; Chang, J. *J. Drug Target.* **2011**, *19*, 373–381.
- [13] Li, X.; Ding, L.; Xu, Y.; Wang, Y.; Ping, Q. *Int. J. Pharm.* **2009**, *373*, 116–123.
- [14] Lee, H.; Hu, M.; Reilly, R.M.; Allen, C. *Mol. Pharm.* **2007**, *4*, 769–781.
- [15] Zhang, J.; Jin, W.; Wang, X.; Wang, J.; Zhang, X.; Zhang, Q. *Mol. Pharm.* **2010**, *7*, 1159–1168.
- [16] Olsen, J.O.; Pozderac, R.V.; Hinkle, G.; Hill, T.; O'Dorisio, T.M.; Schirmer, W.J.; Ellison, E.C.; O'Dorisio, M.S. *Semin. Nucl. Med.* **1995**, *25*, 251–261.
- [17] Engel, J.B.; Schally, A.V.; Dietl, J.; Rieger, L.; Honig, A. *Mol. Pharm.* **2007**, *4*, 652–658.
- [18] Nagy, A.; Schally, A.V.; Halmos, G.; Armatis, P.; Cai, R.Z.; Csernus, V.; Kovacs, M.; Koppan, M.; Szepeshazi, K.; Kahan, Z. *Proc. Natl. Acad. Sci. USA* **1998**, *95*, 1794–1799.
- [19] Huang, C.M.; Wu, Y.T.; Chen, S.T. *Chem. Biol.* **2000**, *7*, 453–461.
- [20] Moody, T.W.; Fuselier, J.; Coy, D.H.; Mantey, S.; Pradhan, T.; Nakagawa, T.; Jensen, R.T. *Peptides* **2005**, *26*, 1560–1566.
- [21] Sun, L.C.; Luo, J.; Mackey, L.V.; Fuselier, J.A.; Coy, D.H. *Cancer Lett.* **2007**, *246*, 157–166.
- [22] Coy, D.H.; Taylor, J. *Metabolism* **1996**, *45*, 21–23.
- [23] Weckbecker, G.; Raulf, F.; Stolz, B.; Bruns, C. *Pharmacol. Ther.* **1993**, *60*, 245–264.
- [24] Yuan, M.; Wang, J.; Deng, J.; Wang, Z.; Yang, W.; Li, G.; Ren, B. *Nucl. Med. Biol.* **2010**, *37*, 317–326.
- [25] Sun, L.C.; Coy, D.H. *Curr. Drug Deliv.* **2011**, *8*, 2–10.
- [26] Morpurgo, M.; Monfardini, C.; Hofland, L.J.; Sergi, M.; Orsolini, P.; Dumont, J.M.; Veronese, F.M. *Bioconj. Chem.* **2002**, *13*, 1238–1243.
- [27] Zhang, Y.; Zhang, H.; Wang, X.; Wang, J.; Zhang, X.; Zhang, Q. *Biomaterials* **2012**, *33*, 679–691.
- [28] Zhao, B.J.; Ke, X.Y.; Huang, Y.; Chen, X.M.; Zhao, X.; Zhao, B.X.; Lu, W.L.; Lou, J.N.; Zhang, X.; Zhang, Q. *J. Drug Target.* **2011**, *19*, 382–390.
- [29] Diaz-Mochon, J.J.; Bialy, L.; Bradley, M. *Org. Lett.* **2004**, *6*, 1127–1129.
- [30] Gaucher, G.; Dufresne, M.H.; Sant, V.P.; Kang, N.; Maysinger, D.; Leroux, J.C. *J. Control. Release* **2005**, *109*, 169–188.
- [31] Vichai, V.; Kirtikara, K. *Nat. Protoc.* **2006**, *1*, 1112–1116.
- [32] Kalchenko, V.; Shvitiel, S.; Malina, V.; Lapid, K.; Haramati, S.; Lapidot, T.; Brill, A.; Harmelin, A. *J. Biomed. Opt.* **2006**, *11*, 050507.
- [33] Mamot, C.; Drummond, D.C.; Noble, C.O.; Kallab, V.; Guo, Z.; Hong, K.; Kirpotin, D.B.; Park, J.W. *Cancer Res.* **2005**, *65*, 11631–11638.
- [34] Riezman, H.; Woodman, P.G.; van Meer, G.; Marsh, M. *Cell* **1997**, *91*, 731–738.
- [35] Yamamoto, Y.; Nagasaki, Y.; Kato, Y.; Sugiyama, Y.; Kataoka, K. *J. Control. Release* **2001**, *77*, 27–38.

- [36] Dubey, V.; Nahar, M.; Mishra, D.; Mishra, P.; Jain, N.K. *J. Drug Target.* **2011**, *19*, 258–269.
- [37] Yang, R.; Meng, F.; Ma, S.; Huang, F.; Liu, H.; Zhong, Z. *Biomacromolecules.* **2011**, *12*, 3047–3055.
- [38] Desmetre, T.; Devoisselle, J.M.; Mordon, S. *Surv. Ophthalmol.* **2000**, *45*, 15–27.
- [39] Kawano, K.; Watanabe, M.; Yamamoto, T.; Yokoyama, M.; Opanasopit, P.; Okano, T.; Maitani, Y. *J. Control. Release.* **2006**, *112*, 329–332.
- [40] Basile, L.; Pignatello, R.; Passirani, C. *Curr. Drug Deliv.* **2012**, *9*, 255–268.

伐普肽修饰的纳米胶束作为递送紫杉醇至生长抑素受体 过表达肿瘤的靶向载体研究

侯文杰, 郑华, 王坚成*

北京大学医学部 药学院 药剂学系, 北京 100191

摘要: 生长抑素受体在肿瘤细胞中有广泛表达。伐普肽(Vapreotide, VAP)作为生长抑素类似物, 因其具有与生长抑素受体高度亲和力而被用作肿瘤靶向递送系统的修饰物。本研究针对伐普肽结构中D-苯丙氨酸的外环 α -NH₂与NHS-PEG-DSPE进行特异性化学偶联得到导向化合物DSPE-PEG-VAP, 并利用其修饰载紫杉醇纳米胶束给药系统。研究表明, 靶向配体修饰和未修饰的两种载药系统具有相似的粒径大小、表面电势、药物包载效率以及药物释放行为。在人乳腺癌MCF-7细胞模型评价中, 靶向组比非靶向组具有更高的细胞摄取量; 体内肿瘤模型中靶向组也表现出较高的肿瘤组织药物蓄积量和更优的肿瘤治疗效应。因此, 我们认为这种伐普肽修饰的纳米胶束将成为向生长抑素受体高表达的肿瘤靶向递送抗肿瘤药物的一种有潜力的载药系统。

关键词: 生长抑素受体; 伐普肽; 靶向纳米胶束; 紫杉醇; 肿瘤治疗